Simulated Siberian snow cover response to observed Arctic sea ice loss, 1979–2008

Debjani Ghatak,[1] Clara Deser,[2] Allan Frei,[3,4] Gavin Gong,[5] Adam Phillips,[2] David A. Robinson,[6] and Julienne Stroeve[7]

Received 7 May 2012; revised 2 October 2012; accepted 11 October 2012; published 7 December 2012.

[1] The loss of Arctic sea ice has wide-ranging impacts, some of which are readily apparent and some of which remain obscure. For example, recent observational studies suggest that terrestrial snow cover may be affected by decreasing sea ice. Here, we examine a possible causal link between Arctic sea ice and Siberian snow cover during the past 3 decades using a suite of experiments with the National Center for Atmospheric Research Community Atmospheric Model version 3. The experiments were designed to isolate the influence of surface conditions within the Arctic Ocean from other forcing agents such as low-latitude sea surface temperatures and direct radiative effects of increasing greenhouse gases. Only those experiments that include the observed evolution of Arctic sea ice and sea surface temperatures result in increased snow depth over Siberia, while those that maintain climatological values for Arctic Ocean conditions result in no snow signal over Siberia. In the former, Siberian precipitation and air temperature both increase, but because surface air temperatures remain below freezing during most months, the snowpack thickens over this region. These results suggest that Arctic Ocean surface forcing is necessary and sufficient to induce a Siberian snow signal, and that other forcings in combination can modulate the strength and geographic extent of the response.

Citation: Ghatak, D., C. Deser, A. Frei, G. Gong, A. Phillips, D. A. Robinson, and J. Stroeve (2012), Simulated Siberian snow cover response to observed Arctic sea ice loss, 1979–2008, *J. Geophys. Res.*, *117*, D23108, doi:10.1029/2012JD018047.

1. Introduction

[2] Changes in the Northern Hemisphere high-latitude environment, including a rapid decline in summer Arctic sea ice cover, are under scrutiny for their impact on global climate [*Hassol*, 2004; *Stroeve et al.*, 2005, 2007; *Comiso et al.*, 2008]. For example, one recent study examines changes in precipitation, evapotranspiration, and river discharge over the terrestrial pan-Arctic region through the analyses of observations and coupled GCM simulations [*Rawlins et al.*, 2010]. They found positive trends in precipitation, evapotranspiration, and river discharge both in observations and in model simulations, suggesting an intensification of the freshwater cycle.

[3] Land-surface snow over the middle and high latitudes has also been changing [*Ye et al.*, 1998; *Clark et al.*, 1999; *Frei and Robinson*, 1999; *Brown*, 2000; *Ye*, 2001; *Ye and Ellison*, 2003; *Ye et al.*, 2003; *Hassol*, 2004; *Iijima et al.*, 2007; *Brown and Mote*, 2009; *Bulygina et al.*, 2009, 2011; *Brown et al.*, 2010; *Fontana et al.*, 2010; *Ghatak et al.*, 2010; *McCabe and Wolock*, 2010]. The response of snow to climatic forcing is complex and depends on the spatial and temporal scales of study. *Biancamaria et al.* [2011] showed a statistically significant negative trend in snow volume (-9.7 ± 3.8 km^3 yr^{-1}, p value = 0.02) over North America and a statistically insignificant positive trend in snow volume (11.3 ± 9.3 km^3 yr^{-1}, p value = 0.25) over Eurasia by analyzing data from the Special Sensor Microwave/Imager (SSM/I) between 1989 and 2006 period. The loss of Northern Hemisphere spring snow cover extent has accelerated during the last 40 years with a rate of decrease of ~0.8 million km^2 per decade [*Brown and Robinson*, 2011]. The diminished spring snow covered area since 1970 is mainly due to the increased winter warming, which has strengthened in recent years [*McCabe and Wolock*, 2010; *Brown and Robinson*, 2011]. Pan-Arctic snow cover extents during May and June have also decreased, 14% and 46% respectively, over the 1967–2008 period due to earlier snowmelt [*Brown et al.*, 2010].

[4] A study based on 110 stations from the Former Soviet Union (FSU) showed that the mean cold season snow depth

[1]Institute of Marine and Coastal Sciences, Rutgers University, New Brunswick, New Jersey, USA.
[2]Global and Climate Dynamics, National Center for Atmospheric Research, Boulder, Colorado, USA.
[3]Department of Geography, Hunter College, New York, New York, USA.
[4]Program in Earth and Environmental Sciences, City University of New York, New York, New York, USA.
[5]Department of Earth and Environmental Engineering, Columbia University, New York, New York, USA.
[6]Department of Geography, Rutgers University, Piscataway, New Jersey, USA.
[7]National Snow and Ice Data Center, University of Colorado Boulder, Boulder, Colorado, USA.

Corresponding author: D. Ghatak, Institute of Marine and Coastal Sciences, Rutgers University, 71 Dudley Rd., New Brunswick, NJ 08901, USA. (ghatak@marine.rutgers.edu)

Table 1. The Forcing Characteristics of the CAM3 Experiments

Experiment Name	Radiative Forcings (Greenhouse Gases, Tropospheric and Stratospheric Ozone, Sulfate and Volcanic Aerosols, and Solar Insolation)	Extra Tropical Surface Forcings (SSTs and Sea Ice Poleward 20°)	Tropical Surface Forcings (SSTs 20°N–20°S)	Time Domain
GHG + SST + ICE	time-varying	time-varying	time-varying	1950–2008
SST + ICE	fixed at 1990 level	time-varying	time-varying	1950–2008
GHG	time-varying	climatological seasonal cycle	climatological seasonal cycle	1950–2008
Tropical SST	fixed at 1990 level	climatological seasonal cycle	time-varying	1950–2009
ICE	fixed at 1990 level	time-varying for sea ice and local SST (see text); climatological seasonal cycle for SSTs elsewhere.	climatological seasonal cycle	1979–2009

was affected by warming in only a few areas during the second half of 20th century [*Fallot et al.*, 1997]. A more recent study of 820 Russian stations with snow measurements between 1966 and 2007 revealed that snow cover duration decreased over the northern regions of European Russia, and increased over central Siberia (Yakutia) and the Far East [*Bulygina et al.*, 2009].

[5] Warming due to increasing greenhouse gases leads to the loss of seasonal snowpacks, which causes a threat to the water supply of one-sixth of the world's population [*Barnett et al.*, 2005]. General circulation model simulations suggest that in response to increasing greenhouse gases, snow water equivalent (SWE) will decrease over most of the mid-latitudinal regions of the Northern Hemisphere, but will increase over the Canadian Arctic and Siberia [*Barry et al.*, 2007; *Räisänen*, 2008]. A recent study based on 11 high-resolution regional model simulations collectively suggest an expected loss of snow water equivalent over Northern Europe during the 21st century; though there are some exceptions (e.g., the mountains of Northern Sweden) [*Räisänen and Eklund*, 2011].

[6] While snow has generally decreased over Eurasia [*Ye et al.*, 2003; *Hassol*, 2004; *Ye et al.*, 2008] during the last half of the 20th century, some areas have experienced more snow [*Bulygina et al.*, 2009, 2011; *Ghatak et al.*, 2010]. *Ghatak et al.* [2010] examined the covariation between observed changes in snow duration (1979–2007) and Arctic sea ice loss, which suggest that snow over Siberia potentially increases with Arctic sea ice loss. According to model, this signal can be expected to strengthen over the next one to 3 decades [*Ghatak et al.*, 2010]. This is consistent with the modeling study by *Deser et al.* [2010]. *Liu et al.* [2012] showed a linkage between retreating Arctic sea ice and winter snowfall over both the continents of North America and Eurasia.

[7] Here, we investigate a possible causal linkage between Siberian snow and sea ice using a suite of modeling experiments, the objective of which is to isolate the impact of changing sea ice from other forcings. Details of the experiments are discussed in section 2, results are shown in section 3 and conclusions are discussed in section 4.

2. Experiments and Methodology

[8] We use the National Center for Atmospheric Research (NCAR) Community Atmospheric Model version 3 (CAM3) coupled to the Community Land Model (CLM), which are the atmospheric and terrestrial components of the Community Climate System model version 3 (CCSM3), respectively. These models are described in detail by *Collins et al.* [2006] and references therein. The strengths and weaknesses of CAM3 in simulating the mean state and interannual variability are reported by *Hurrell et al.* [2006].

[9] We analyze results from a suite of five CAM3/CLM experiments, which have been specifically designed to isolate the impacts of Arctic Sea Surface Temperature (SST) and sea ice changes from other forcings (discussed below). These experiments have been performed at T42 horizontal resolution (approximately 2.8° of latitude and 2.8° of longitude). Each of the 5 experiments consists of five ensemble members each of which begins from different atmospheric initial conditions. We present results for the average of five ensemble members.

[10] For these experiments we group boundary forcings into two categories: radiative and surface. Radiative boundary forcings include atmospheric chemical composition (greenhouse gases, tropospheric and stratospheric ozone, sulfate and volcanic aerosols) and their associated radiative impacts as well as solar insolation variations. Surface boundary forcings include global SST and sea ice concentration variations. The differences between the experiments are whether or not they include the time-evolving observed values for these forcings. When the time-varying radiative boundary forcings are not included, they are maintained at 1990 levels to approximate conditions during the late 20th century. When the time-varying surface boundary forcings are not included, the mean seasonal cycle is repeated during each year of the experiment. The *Hurrell et al.* [2006] data set has been used for the SST and sea ice concentrations.

[11] Table 1 summarizes the forcings included in each of the five experiments denoted as "GHG+SST+ICE," "SST+ICE," "ICE," "GHG" and "Tropical SST." The "GHG+SST+ICE" experiment is forced by all observed, time-evolving boundary conditions, including both radiative and surface. "SST+ICE" is forced by global time-evolving surface boundary conditions and constant radiative forcing. "ICE" is forced by time-varying Arctic sea ice concentrations, with climatological values for the other surface forcing components with the exception of SSTs within grid boxes partially covered by ice. In these regions, we have incorporated the local, direct effect of ice loss on SST (e.g., when there is less ice, there is more incident solar radiation at the sea surface which heats the ocean mixed layer) by including time-varying SSTs in those grid boxes and months when the sea ice concentration is less than the climatological value by at least 10% (see *Screen et al.* [2012b] for additional details). "GHG" is forced by the observed evolution of radiative forcings [*Meehl et al.*, 2006], with climatological values for the mean seasonal

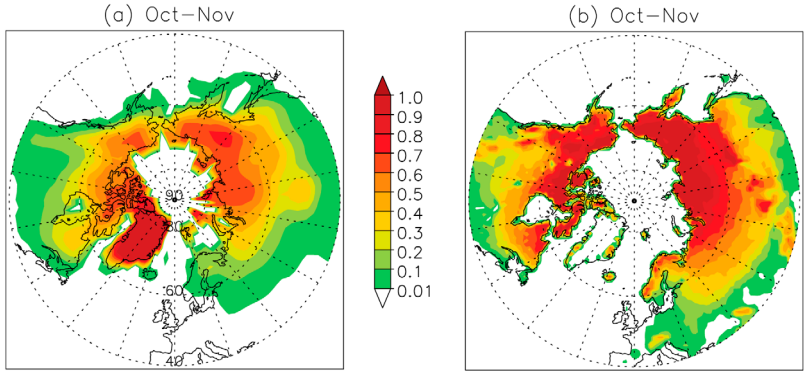

Figure 1. Climatology (1979–2007) of autumn (October–November) fractional snow cover (%) from (a) the "GHG + SST + ICE" CAM3 experiment and (b) observations.

cycle of SSTs and sea ice. "Tropical SST" is forced by the observed evolution of SSTs in the tropics (20°N–20°S), with climatological values elsewhere. More details of these experiments are provided by *Deser and Phillips* [2009] and also can be found online at http://www.cesm.ucar.edu/working_groups/Climate/experiments/ccsm3.0/.

[12] The temporal domain of our analyses is restricted to October through March, 1979/1980–2007/2008, which coincides with the period of regular satellite observations of sea ice from passive microwave observations. This helps us to understand how the historic simulations can be compared with the observed variability. The spatial domain of our analysis is limited to the Arctic Ocean and Eurasia north of 45°N. We present results at bimonthly time scale, i.e., October–November (ON), December–January (DJ) and February–March (FM).

[13] The variables analyzed include monthly mean snow depth ('SNOWDP' in meters), lowest model level water vapor mixing ratio ('QBOT' in gm/kg), surface air temperature ('SAT' in °C), precipitation ('PRECIP' in mm/d) and snowfall ('SNF' in mm/d). Linear regression analysis has been employed between the September sea ice extent time series (SIE) (available from NSIDC's Sea Ice Index, http://nsidc.org/data/seaice_index) and each of the variables. Because the SIE has a negative trend, the resulting regression coefficients are displayed with reversed sign so that positive values represent increases in the regressed variable as SIE decreases. Similar results are obtained with linear trend analysis (not shown). We assess the 5% statistical significance of the regression coefficients following a Student's t test [*Helsel and Hirsch*, 1992]. Although we present regression coefficients at each grid cell, we discuss only those features that show significant values over large geographical areas.

[14] As context for the regression analysis, Figure 1 shows climatological October–November snow cover conditions from the "GHG + SST + ICE" model experiment and from observations. Snow cover extent (fraction of land covered by snow) is shown for the model as well as from observations [*Armstrong and Brodzik*, 2005]. EASE grid (Equal Area Scalable Earth Grid) snow extent data [*Armstrong and Brodzik*, 2005] based on NOAA-NESDIS snow charts has been obtained from the National Snow and Ice Data Center (NSIDC). Please note that Figures 1a and 1b have different spatial resolution. A visual comparison indicates that the spatial patterns match well, with larger values over high latitudes and over mountainous regions (compare Figures 1a and 1b).

3. Results

[15] Regression analyses between September SIE and SNOWDP in the following ON, DJ and FM show that loss of September SIE is associated with an increase in SNOWDP over central and eastern Siberia (over the northern Yenisey and Lena river basins) in the "GHG + SST + ICE," "SST + ICE" and "ICE" experiments (Figure 2). Significant increases in SNOWDP are observed during DJ and FM in the "GHG + SST + ICE" and "SST + ICE" experiments and during ON, DJ and FM in "ICE" experiment. In the two experiments without time-varying Arctic surface boundary forcings ("GHG" and "Tropical SST"), no significant signal in SNOWDP emerges over this region (not shown). Results from individual ensemble members (not shown) exhibit similar Siberian snow depth signals, though the geographical extent and statistical significance of this association vary slightly among them.

[16] Another noticeable pattern is found over western Eurasia, where retreating September SIE is followed by significantly decreasing SNOWDP during October through March over the region extending from Scandinavia to the Ob river basin in both "GHG + SST + ICE" and "SST + ICE" experiments (Figure 2). This signal is not apparent in the "ICE" experiment. The "GHG" and "Tropical SST" experiments show no coherent and consistent signal except over central Russia in "Tropical SST" (not shown).

[17] To understand the snow depth signals, we examine regression maps between September SIE and subsequent SAT (Figure 3), QBOT (Figure 4), PRECIP (Figure 5) and SNF (Figure 6). Reduced September SIE is followed by statistically significant warming over the Pacific sector of the Arctic Ocean and over the adjacent Eurasian landmass including Siberia in all three experiments, mainly during ON (Figures 3a–3c). The strongest response is found over the East Siberian, Chukchi and Laptev Seas which coincides with the area of recent observed summer ice loss. In the "ICE" experiment, this signal does not persist into DJ and FM. In other experiments, the ON signal is more extensive than "ICE" experiment, and persists in some form through

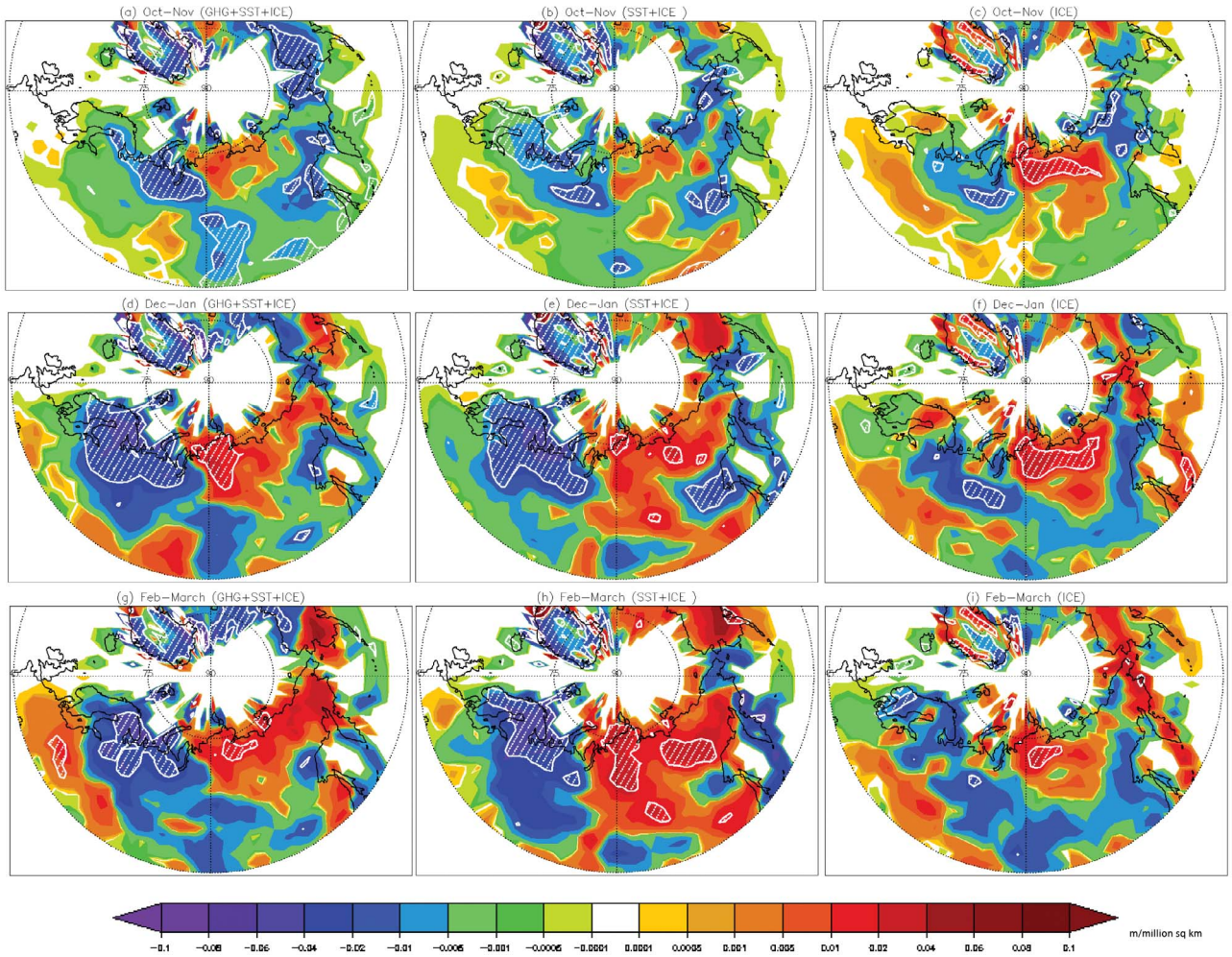

Figure 2. Regression coefficients ($m/10^6$ km^2) of bimonthly SNOWDP upon September SIE during 1979–2008 for the "GHG + SST + ICE," "SST + ICE" and "ICE" experiments in (a–c) October–November; (d–f) December–January; and (g–i) February–March. Regression coefficients are plotted with reversed sign to denote conditions associated with ice loss. Regression coefficients significant at the 5% confidence level are indicated by the white contours and shading.

March (Figure 3). Neither of the experiments that exclude time-varying Arctic surface boundary forcing exhibit significant Siberian warming (not shown).

[18] These analyses indicate that September Arctic sea ice loss and associated local SST increases cause ON warming of surface air temperatures both over the Arctic Ocean and over adjacent land surfaces, consistent with previous observational studies [*Serreze et al.*, 2009; *Screen and Simmonds*, 2010] and modeling experiments [*Deser et al.*, 2010; *Kumar et al.*, 2010; *Screen et al.*, 2012b]. Our results indicate that while SIE alone can cause such a response, other forcings in tandem with SIE can result in a spatial pattern similar to what has been observed [e.g., see *Serreze et al.*, 2009, Figure 3b; *Screen et al.*, 2012a].

[19] Response of QBOT to the loss of September Arctic SIE during ON, DJ and FM is similar to the responses of SAT (compare Figures 3 and 4). Figures 4a–4c confirm an increase in moisture over the Arctic Ocean and over Siberia mainly during ON in all three experiments, which is intuitive from significant warming as seen in Figures 3a–3c over the same region. The increased QBOT in the atmosphere provides a mechanism for increased precipitation and snowfall in this region associated with changing sea ice conditions.

[20] Therefore, we investigate whether this model shows the expected precipitation changes. In fact, a decrease in September SIE is associated with a significant increase in precipitation over the Arctic Ocean and adjacent Siberia during ON in the experiments with time-varying sea ice forcing (Figures 5a–5c). The experiments without time-varying sea ice forcing show no such signal (not shown). There is some persistence of the significantly increased precipitation signal into DJ in the "GHG + SST + ICE" and "SST + ICE" experiments, but not in the "ICE" experiment.

[21] There are other regions with significant precipitation responses that are unique to each of the five experiments. For example, in "GHG + SST + ICE," precipitation increases over the western North Pacific Ocean and over eastern Eurasia during DJ and FM associated with retreating summer SIE (Figures 5d and 5g). In "SST + ICE," we find a FM precipitation signal that is mainly centered over the Arctic

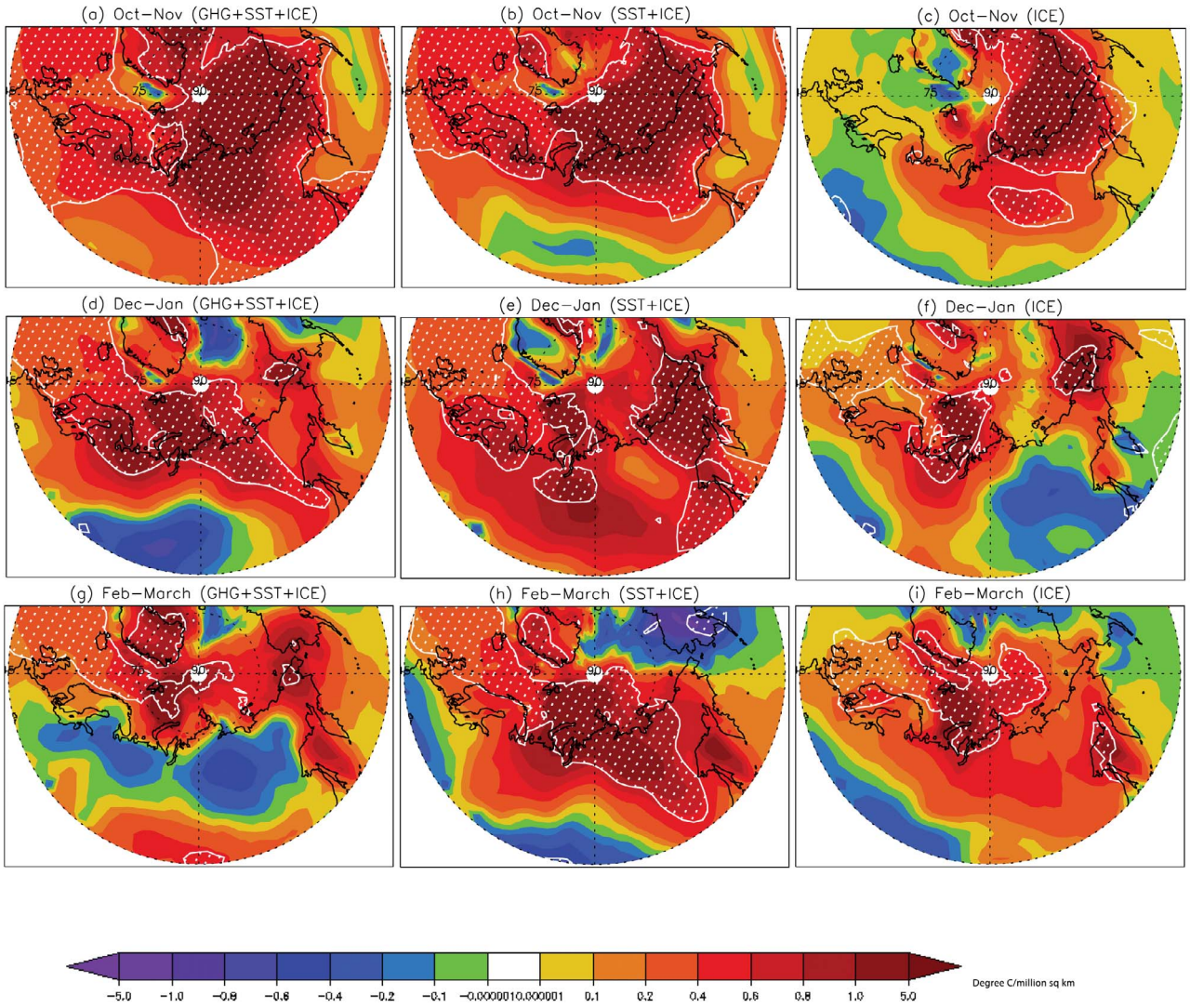

Figure 3. As in Figure 2 but for SAT (°C/10^6 km^2).

Ocean and over the Eurasian landmasses (Figure 5h). Regression plots for the Tropical SST experiment (not shown) show an increase in precipitation over the North Pacific and a decrease over part of Eurasia during DJ following summer SIE loss. A more detailed discussion of these changes is beyond the scope of this manuscript.

[22] Regression patterns of snowfall are consistent with the precipitation patterns (compare Figures 5 and 6). The experiments with time-varying sea ice forcing show an increase in snowfall associated with decreasing sea ice over the Arctic Ocean and over adjacent Siberia during ON (Figures 6a–6c). Furthermore, a decrease in snowfall is found over western Eurasia during ON and DJ in "GHG+SST+ICE" experiment and during ON in "SST+ICE" experiment.

[23] Regional time series of SAT and PRECIP over Siberia (60°N–75°N, 95°E–135°E) are shown in Figure 7. This region coincides with the area where a loss of September SIE corresponds to an increase in SNOWDP (recall Figure 2). Temperature trends over Siberia appear, at first glance, to be related to radiative and SST forcing, but not to sea ice forcing: significant temperature trends are found only in those experiments where ice forcing is complemented by other forcings (Table 2). However, this may be due to the fact that, while the other forcings have trends during the entire period of this analysis, the sea ice forcing becomes strong only after 2000. Figure 7 shows that during the more recent period, Siberian temperature and precipitation both increase in concert with decreasing sea ice extent. In experiments without time-varying sea ice forcing, no significant trend is found with the exception of "GHG" during DJ (Table 2).

[24] In the experiments with time-varying sea ice forcing, precipitation trends over Siberia are significant and positive during ON (Table 2). In those without sea ice forcing, no significant precipitation trends are found over Siberia during this season. There is no indication that sea ice alone is related to precipitation variations in December through March.

[25] As a result of these temperature and precipitation signals, we find statistically significant positive trends in Siberian snow depth in "GHG+SST+ICE" during DJ and FM; in "SST+ICE" during FM; and in "ICE" during ON (Table 2). Despite the positive temperature trends over

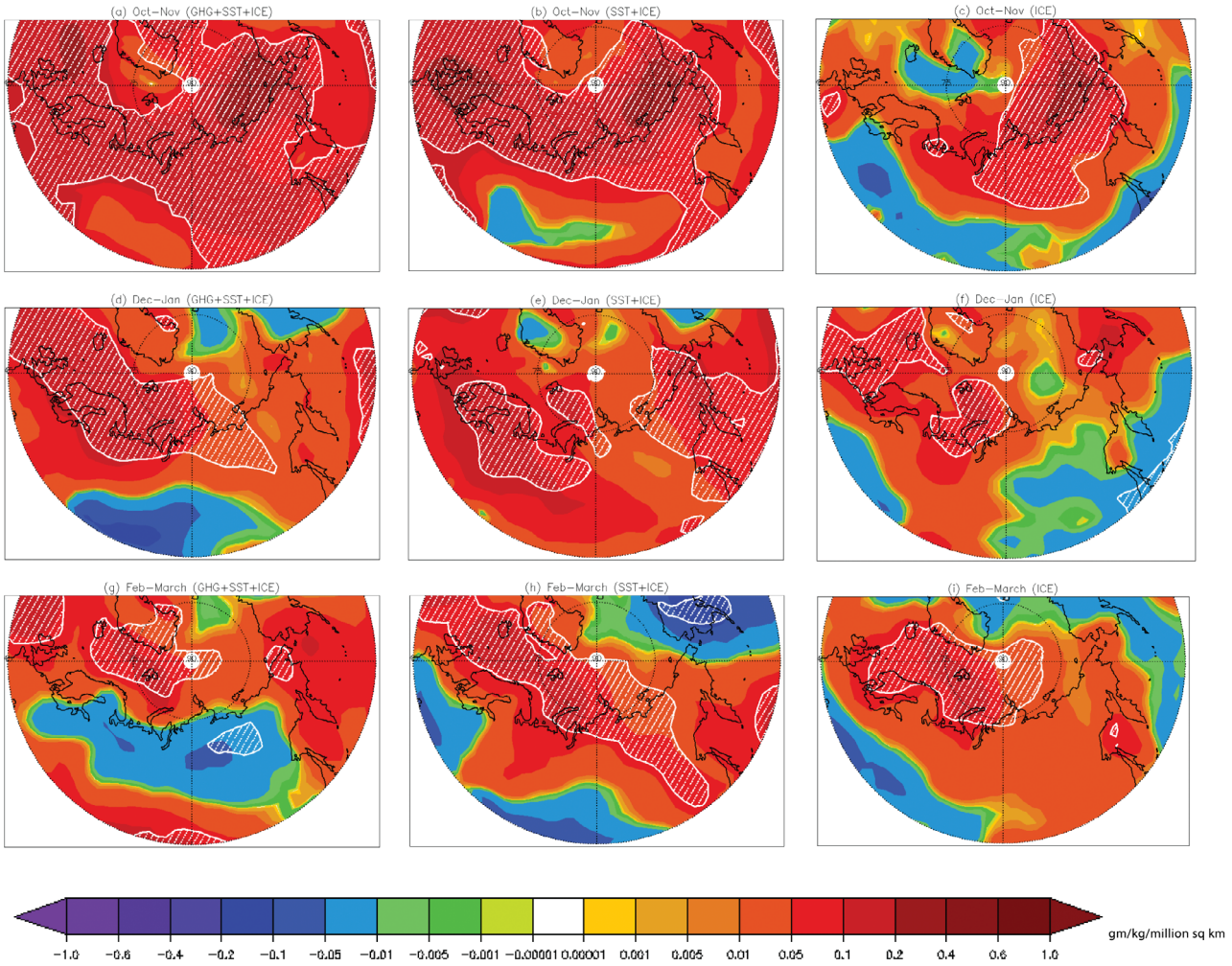

Figure 4. As in Figure 2 but for QBOT (gm/kg/10^6 km^2).

Siberia, monthly average temperatures remain below −10°C (Figure 7a), resulting in atmospheric conditions that remain favorable for precipitation falling as snow (Figure 6), and for the persistence of snow on the ground. This explains why the trend in SNOWDP becomes stronger during FM in "GHG+SST+ICE" and "SST+ICE," as is observed in Figure 2 as well. Synergistic effects between SST and sea ice trends may result in an extension of the duration of the SNOWDP signal into late winter in these experiments compared to the "ICE" experiment, but further investigation is needed to substantiate this claim. In the "GHG" and "Tropical SST" experiments, we find no significant trend in Siberian SNOWDP in any season (Table 2).

4. Conclusions and Discussion

[26] We have presented results from a suite of five CAM3/CLM experiments designed to isolate the impact of changes in sea ice and SSTs in the Arctic Ocean and marginal seas on Siberian snow cover. The experiments include two groups of forcings—radiative and surface boundary—in different combinations. Snow depth is found to increase over central and eastern Siberia following summer sea ice loss only in those experiments which include time-varying Arctic sea ice and SSTs (e.g., "GHG+SST+ICE," "SST+ICE" and "ICE"): the other experiments show no such signal. This leads us to conclude that, according to the CAM3/CLM model, Arctic surface boundary forcing plays a major role in generating this Siberian snow increase. These results are consistent with the observational findings of *Ghatak et al.* [2010] which show an empirical connection between summer Arctic sea ice loss and autumn/early winter snow cover duration over Siberia.

[27] Statistically significant warming is found over the Arctic Ocean as well as over Siberia. This suggests a positive feedback in which the loss of summer sea ice results in atmospheric surface level warming over the Arctic Ocean and Eurasia. These results are consistent with the recent warming observed over the Arctic primarily during autumn [*Serreze et al.*, 2009; *Screen and Simmonds*, 2010]. This suite of experiments suggests that the effect of sea ice variations on temperature, water vapor content, precipitation and snowfall over the Arctic Ocean and Siberia is most extensive during ON. *Stroeve et al.* [2011] suggest more frequent and intensified cyclones over the Atlantic sector of the Arctic during years of low sea ice; this leads to an

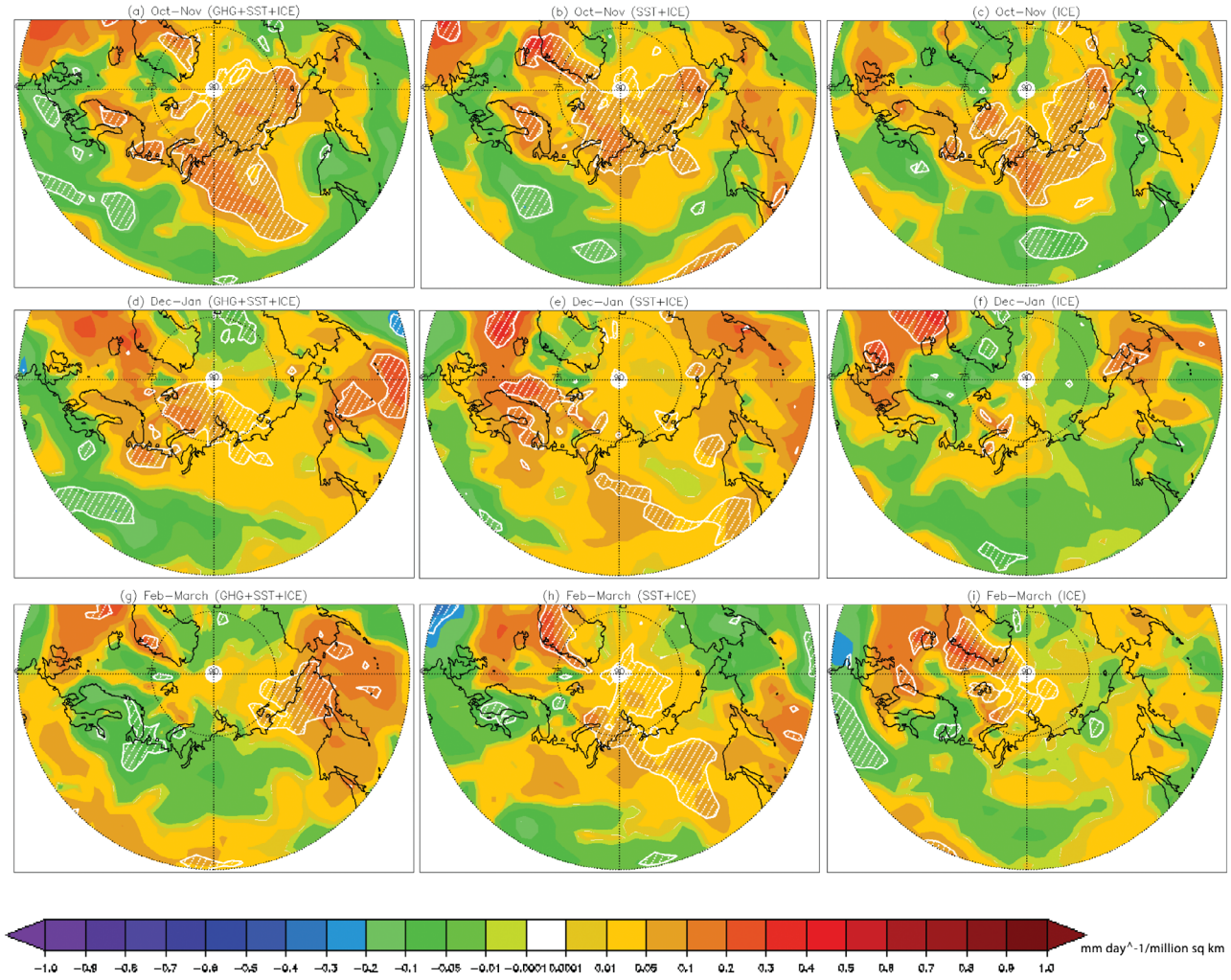

Figure 5. As in Figure 2 but for PRECIP (mm $d^{-1}/10^6$ km^2).

increase in autumn cyclone associated precipitation, which is also apparent over Eurasia. *Screen and Simmonds* [2012] also showed an increase in Arctic precipitation in September–October–November.

[28] Increased snow cover over Siberia in these three experiments is caused by increased surface air temperature and precipitation during ON. The temperature connection may seem counterintuitive, but in a scenario with significant warming, when average monthly temperatures remain below freezing during the snow season, as they do in this region, conditions are favorable for increased snowfall and more persistent snow on ground. Atmospheric warming over these regions increases the availability of moisture, facilitating increased snow fall and a deeper snowpack over Siberia.

[29] In the experiment with only Arctic Ocean surface forcing, the snow signal over Siberia is apparent. In the two other experiments that include Arctic Ocean surface forcings plus other surface and radiative forcings, the signal is more geographically extensive during winter. In the experiments with no Arctic Ocean surface forcing, no Siberian snow signal is apparent. Thus, Arctic Ocean surface forcing is necessary and sufficient to produce a Siberian snow signal, but other surface and radiative boundary forcings can modulate the magnitude and geographic extent of the signal.

[30] It should be noted that our conclusions are based solely on CAM3/CLM simulations and thus may be model-dependent. For example, a recent study that performed similar "ICE" experiments with the UK-Australian Unified Model version 7.3 (UM7.3) finds considerably weaker fall/winter warming over Siberia in UM7.3 compared to CAM3 as well as somewhat different precipitation responses [*Screen et al.*, 2012b].

[31] This study addresses one aspect of a feedback cycle that has previously been identified in the high-latitude climate system. Other studies have established a remote teleconnection between autumn Siberian snow cover and the following winter's Northern Annular Mode atmospheric circulation pattern [*Gong et al.*, 2003; *Fletcher et al.*, 2009; *Cohen et al.*, 2012]. In fact, a statistical model using October mean snow cover was able to generate a better forecast of the winter air temperature over the extra-tropical Northern Hemisphere than a dynamical forecast system [*Cohen and Fletcher*, 2007]. Our study contributes to our understanding of the large-scale feedback system by explaining the response of fall snow to the loss of summer sea ice loss. It is hoped that additional examination of these model results will shed more light on the physical mechanisms responsible for the relationships identified in this study.

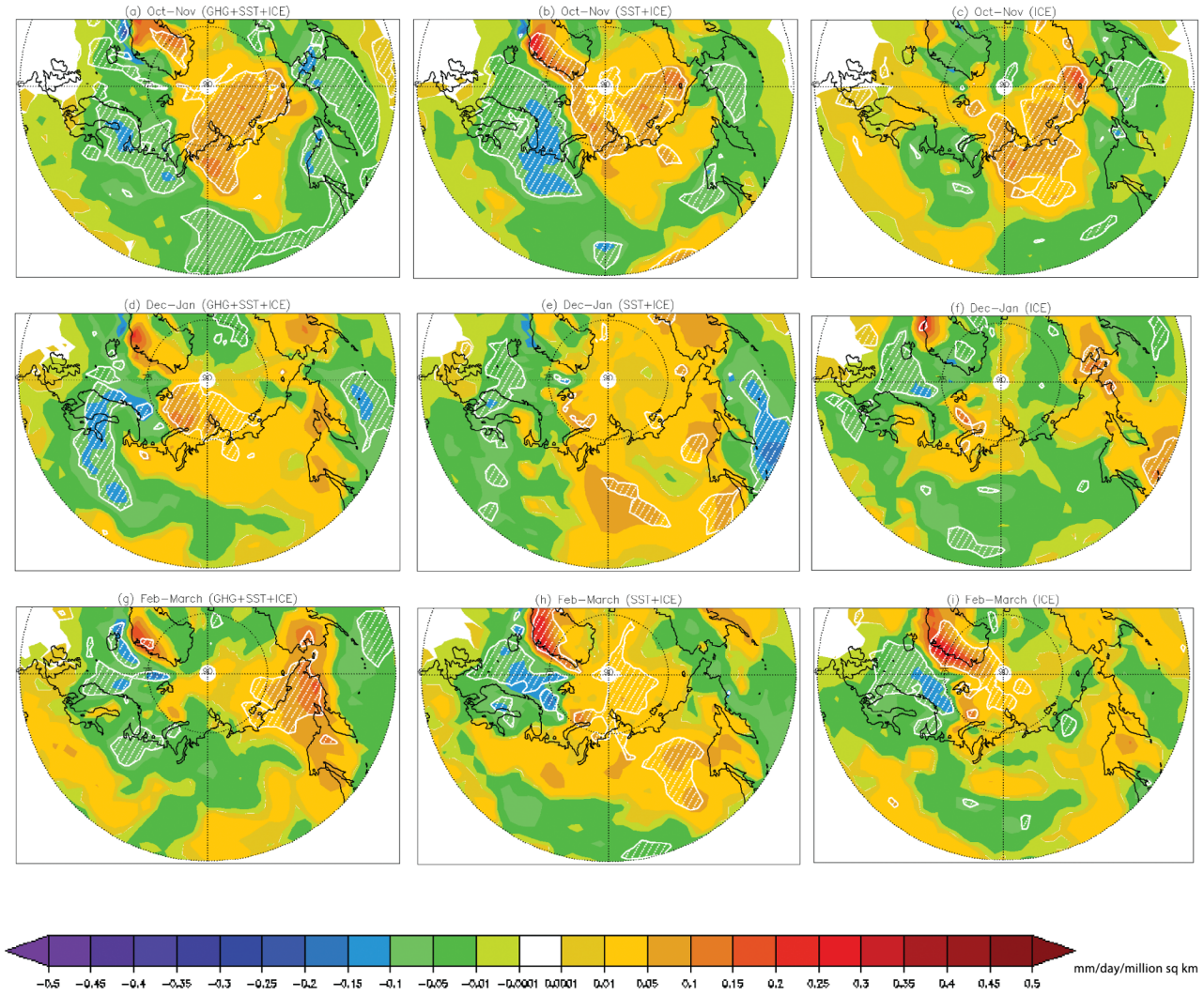

Figure 6. As in Figure 2 but for SNF (mm $d^{-1}/10^6$ km^2).

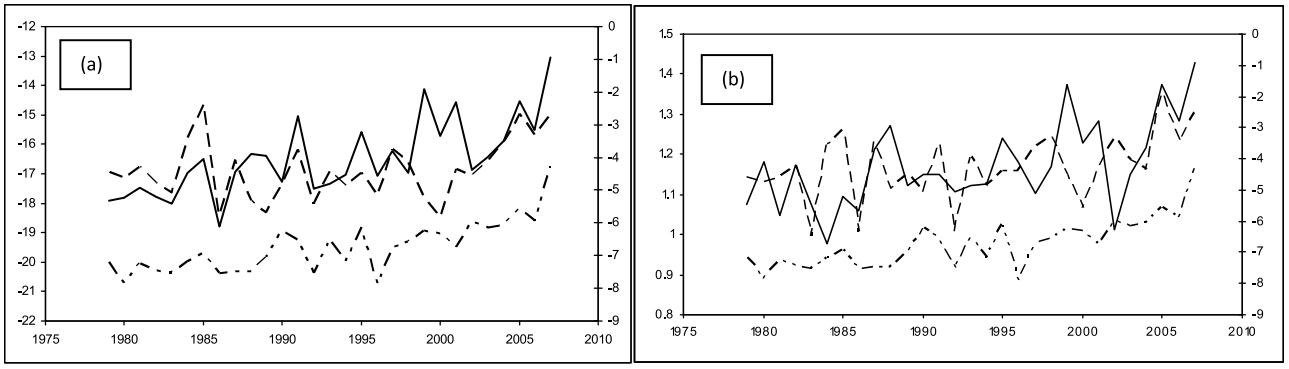

Figure 7. Time series of October–November (a) SAT and (b) PRECIP over Siberia (60°N–75°N and 95°E–135°E) from "GHG+SST+ICE" (solid line) and "ICE" (dashed line) superimposed upon the observed September SIE time series (dashed dotted line). The *y* axis scale on the left in Figure 7a indicates SAT (°C) and in Figure 7b indicates PRECIP (mm/d). The *y* axis scale on the right of both indicates sea ice extent (million sq km). Note that sea ice extent is plotted with reversed sign.

Table 2. Linear Trend Coefficients for Seasonal Surface Air Temperature (SAT, °C/Decade), Precipitation (PRECIP, mm/Day/Decade), and Snow Depth (SNOWDP, cm/Decade) Over Siberia Between 1979 and 2008[a]

	October–November			December–January			February–March		
	SAT	PRECIP	SNOWDP	SAT	PRECIP	SNOWDP	SAT	PRECIP	SNOWDP
GHG+SST+ICE	**1.09 (0.000)**	**0.07 (0.001)**	0.29 (0.281)	**0.73 (0.003)**	0.02 (0.057)	**0.96 (0.014)**	−0.04 (0.873)	5.50E-04 (0.971)	**1.04 (0.017)**
SST+ICE	**0.80 (0.005)**	**0.05 (0.010)**	0.05 (0.862)	**0.54 (0.053)**	0.01 (0.289)	0.71 (0.090)	**0.98 (0.001)**	**0.05 (0.007)**	**1.29 (0.009)**
ICE	0.34 (0.135)	**0.04 (0.025)**	**0.70 (0.033)**	−0.04 (0.894)	−0.01 (0.587)	0.69 (0.068)	0.41 (0.081)	−0.01 (0.620)	0.24 (0.548)
GHG	0.16 (0.379)	0.000 (0.865)	−0.25 (0.362)	**0.51 (0.053)**	**0.03 (0.053)**	0.03 (0.933)	0.11 (0.699)	−0.01 (0.545)	0.29 (0.385)
Tropical SST	0.25 (0.131)	0.01 (0.407)	−0.13 (0.653)	−0.17 (0.546)	**−0.02 (0.052)**	−0.22 (0.594)	−0.16 (0.503)	0.000 (0.919)	−0.34 (0.461)

[a]Significance levels are shown in parentheses; values in bold are significant at $p < 0.05$ (at least 5% confidence).

[32] **Acknowledgments.** This work has been supported by the NASA Cryospheric Sciences Division (NNX08AQ70G), NASA MEaSUREs award NNXO8AP34A, and NOAA grant NA08OAR4310678. Part of the funding for Debjani Ghatak came from an Institute of Marine and Coastal Sciences postdoctoral fellowship. James Miller is thanked for helpful discussions. NCAR is sponsored by the National Science Foundation. C. Deser gratefully acknowledges support from the NSF Office of Polar Programs. We thank the reviewers for their constructive comments, which improved the quality of the manuscript.

References

Armstrong, R. L., and M. J. Brodzik (2005), Northern Hemisphere EASE-Grid weekly snow cover and sea ice extent, version 3, Oct. 1966 to Oct. 1978, http://nsidc.org/data/nsidc-0046.html, Natl. Snow and Ice Data Cent., Boulder, Colo.

Barnett, T. P., J. C. Adam, and D. P. Lettenmaier (2005), Potential impacts of a warming climate on water availability in snow dominated regions, *Nature*, *438*, 303–309, doi:10.1038/nature04141.

Barry, R. G., R. Armstrong, T. Callaghan, J. Cherry, S. Gearhead, A. Nolin, D. Russell, and C. Zöckler (2007), Snow, in *Global Outlook for Ice and Snow*, edited by J. Eamer, pp. 39–62, U. N. Environ. Programme, Nairobi.

Biancamaria, S., A. Cazenave, N. M. Mognard, W. Llovel, and F. Frappart (2011), Satellite-based high latitude snow volume trend, variability and contribution to sea level over 1989/2006, *Global Planet. Change*, *75*, 99–107, doi:10.1016/j.gloplacha.2010.10.011.

Brown, R. D. (2000), Northern Hemisphere snow cover variability and change, 1915–1997, *J. Clim.*, *13*(13), 2339–2355, doi:10.1175/1520-0442(2000)013<2339:NHSCVA>2.0.CO;2.

Brown, R. D., and P. W. Mote (2009), The response of Northern Hemisphere snow cover to a changing climate, *J. Clim.*, *22*, 2124–2145, doi:10.1175/2008JCLI2665.1.

Brown, R. D., and D. A. Robinson (2011), Northern Hemisphere spring snow cover variability and change over 1922–2010 including an assessment of uncertainty, *Cryosphere*, *5*, 219–229, doi:10.5194/tc-5-219-2011.

Brown, R., C. Derksen, and L. Wang (2010), A multidata set analysis of variability and change in Arctic spring snow cover extent, 1967–2008, *J. Geophys. Res.*, *115*, D16111, doi:10.1029/2010JD013975.

Bulygina, O. N., V. N. Razuvaev and N. N. Korshunova (2009), Changes in snow cover over northern Eurasia in the last few decades, *Environ. Res. Lett.*, *4*, 045026, doi:10.1088/1748-9326/4/4/045026.

Bulygina, O. N., P. Y. Groisman, V. N. Razuvaev, and N. N. Korshunova (2011), Changes in snow cover characteristics over northern Eurasia since 1966, *Environ. Res. Lett.*, *6*, 045204, doi:10.1088/1748-9326/6/4/045204.

Clark, M. P., M. C. Serreze, and D. A. Robinson (1999), Atmospheric control on Eurasian snow extent, *Int. J. Climatol.*, *19*, 27–40, doi:10.1002/(SICI)1097-0088(199901)19:1<27::AID-JOC346>3.0.CO;2-N.

Cohen, J., and C. Fletcher (2007), Northern Hemisphere winter surface temperature predictions based on land-atmosphere fall anomalies, *J. Clim.*, *20*(16), 4118–4132, doi:10.1175/JCLI4241.1.

Cohen, J., J. C. Furtado, M. A. Barlow, V. A. Alexeev, and J. E. Cherry (2012), Arctic warming, increasing fall snow cover and widespread boreal winter cooling, *Environ. Res. Lett.*, *7*, 014007, doi:10.1088/1748-9326/7/1/014007.

Collins, W. D., et al. (2006), The Community Climate System Model version 3 (CCSM3), *J. Clim.*, *19*, 2122–2143, doi:10.1175/JCLI3761.1.

Comiso, J. C., C. L. Parkinson, R. Gersten, and L. Stock (2008), Accelerated decline in the Arctic sea ice cover, *Geophys. Res. Lett.*, *35*, L01703, doi:10.1029/2007GL031972.

Deser, C., and A. S. Phillips (2009), Atmospheric circulation trends, 1950–2000: The relative roles of sea surface temperature forcing and direct atmospheric radiative forcing, *J. Clim.*, *22*, 396–413, doi:10.1175/2008JCLI2453.1.

Deser, C., R. Tomas, M. Alexander, and D. Lawrence (2010), The seasonal atmospheric response to projected Arctic Sea ice loss in the late twenty-first century, *J. Clim.*, *23*, 333–351, doi:10.1175/2009JCLI3053.1.

Fallot, J.-M., R. G. Barry, and D. Hoogstrate (1997), Variations of mean cold season temperature precipitation and snow depths during the last 100 years in the former Soviet Union, *Hydrol. Sci. J.*, *42*, 301–327, doi:10.1080/02626669709492031.

Fletcher, C. G., S. C. Hardiman, P. J. Kushner, and J. Cohen (2009), The dynamical response to snow cover perturbations in a large ensemble of atmospheric GCM integrations, *J. Clim.*, *22*, 1208–1222, doi:10.1175/2008JCLI2505.1.

Fontana, F. M. A., A. P. Trishchenko, Y. Luo, K. V. Khlopenkov, S. U. Nussbaumer, and S. Wunderle (2010), Perennial snow and ice variations (2000–2008) in the Arctic circumpolar land area from satellite observations, *J. Geophys. Res.*, *115*, F04020, doi:10.1029/2010JF001664.

Frei, A., and D. A. Robinson (1999), Northern Hemisphere snow extent: Regional variability 1972–1994, *Int. J. Climatol.*, *19*, 1535–1560, doi:10.1002/(SICI)1097-0088(19991130)19:14<1535::AID-JOC438>3.0.CO;2-J.

Ghatak, D., A. Frei, G. Gong, J. C. Stroeve, and D. Robinson (2010), On the emergence of an Arctic amplification signal in terrestrial Arctic snow extent, *J. Geophys. Res.*, *115*, D24105, doi:10.1029/2010JD014007.

Gong, G., D. Entekhabi, and J. Cohen (2003), Modeled Northern Hemisphere winter climate response to realistic Siberian snow anomalies, *J. Clim.*, *16*, 3917–3931, doi:10.1175/1520-0442(2003)016<3917:MNHWCR>2.0.CO;2.

Hassol, S. J. (2004), *Impacts of a Warming Arctic: Arctic Climate Impact Assessment*, 139 pp., Cambridge Univ. Press, Cambridge, U. K.

Helsel, D. R., and R. M. Hirsch (1992), *Studies in Environmental Science—Statistical Methods in Water Resources*, 522 pp., Elsevier, Amsterdam.

Hurrell, J. W., J. J. Hack, A. S. Phillips, J. Caron, and J. Yi (2006), The dynamical simulation of the Community Atmosphere Model version 3 (CAM3), *J. Clim.*, *19*, 2162–2183, doi:10.1175/JCLI3762.1.

Iijima, Y., K. Masuda, and T. Ohata (2007), Snow disappearance in eastern Siberia and its relationship to atmospheric influences, *Int. J. Climatol.*, *27*, 169–177, doi:10.1002/joc.1382.

Kumar, A., J. Perlwitz, J. Eischeid, X. Quan, T. Xu, T. Zhang, M. Hoerling, B. Jha, and W. Wang (2010), Contribution of sea ice loss to Arctic amplification, *Geophys. Res. Lett.*, *37*, L21701, doi:10.1029/2010GL045022.

Liu, J., J. A. Curry, H. Wang, M. Song, and R. M. Horton (2012), Impact of declining Arctic sea ice on winter snowfall, *Proc. Natl. Acad. Sci. U. S. A.*, doi:10.1073/pnas.1114910109, in press.

McCabe, G. J., and D. M. Wolock (2010), Long-term variability in Northern Hemisphere snow cover and associations with warmer winters, *Clim. Change*, *99*(1–2), 141–153, doi:10.1007/s10584-009-9675-2.

Meehl, G. A., W. M. Washington, B. D. Santer, W. D. Collins, J. M. Arblaster, A. Hu, D. M. Lawrence, H. Teng, L. E. Buja, and W. G. Strand (2006), Climate change projections for the twenty-first century and climate change commitment in the CCSM3, *J. Clim.*, *19*, 2597–2616, doi:10.1175/JCLI3746.1.

Räisänen, J. (2008), Warmer climates: Less or more snow?, *Clim. Dyn.*, *30*, 307–319, doi:10.1007/s00382-007-0289-y.

Räisänen, J., and J. Eklund (2011), 21st century changes in snow climate in northern Europe as simulated by regional climate models in the ENSEMBLES project: A high-resolution view from ENSEMBLES regional climate models, *Clim. Dyn.*, *38*, 2575–2591, doi:10.1007/s00382-011-1076-3.

Rawlins, M. A., et al. (2010), Analysis of the Arctic system for freshwater cycle intensification: Observations and expectations, *J. Clim.*, *23*, 5715–5737, doi:10.1175/2010JCLI3421.1.

Screen, J. A., and I. Simmonds (2010), The central role of diminishing sea ice in recent Arctic temperature amplification, *Nature*, *464*, 1334–1337, doi:10.1038/nature09051.

Screen, J., and I. Simmonds (2012), Declining summer snowfall in the Arctic: Causes, impacts and feedbacks, *Clim. Dyn.*, *38*, 2243–2256, doi:10.1007/s00382-011-1105-2.

Screen, J. A., C. Deser, and I. Simmonds (2012a), Local and remote forcing of observed Arctic warming, *Geophys. Res. Lett.*, *39*, L10709, doi:10.1029/2012GL051598.

Screen, J. A., I. Simmonds, C. Deser, and R. Tomas (2012b), The atmospheric response to three decades of observed Arctic sea ice loss, *J. Clim.*, doi:10.1175/JCLI-D-12-00063.1, in press.

Serreze, M. C., A. P. Barrett, J. C. Stroeve, D. N. Kindig, and M. M. Holland (2009), The emergence of surface-based Arctic amplification, *Cryosphere*, *3*, 11–19, doi:10.5194/tc-3-11-2009.

Stroeve, J. C., M. C. Serreze, F. Fetterer, T. Arbetter, W. Meier, J. Maslanik, and K. Knowles (2005), Tracking the Arctic's shrinking ice cover: Another extreme September minimum in 2004, *Geophys. Res. Lett.*, *32*, L04501, doi:10.1029/2004GL021810.

Stroeve, J., M. M. Holland, W. Meier, T. Scambos, and M. C. Serreze (2007), Arctic sea ice decline: Faster than forecast, *Geophys. Res. Lett.*, *34*, L09501, doi:10.1029/2007GL029703.

Stroeve, J. C., M. C. Serreze, A. Barrett, and D. N. Kindig (2011), Attribution of recent changes in autumn cyclone associated precipitation in the Arctic, *Tellus, Ser. A*, *63*(4), 653–663, doi:10.1111/j.1600-0870.2011.00515.x.

Ye, B., D. Yang, and D. L. Kane (2003), Changes in Lena river streamflow hydrology: Human impacts vs. natural variations, *Water Resour. Res.*, *39*(7), 1200, doi:10.1029/2003WR001991.

Ye, H. (2001), Increases in snow season length due to earlier first snow and later last snow dates over north central and northwest Asia during 1937–94, *Geophys. Res. Lett.*, *28*(3), 551–554, doi:10.1029/2000GL012036.

Ye, H., and M. Ellison (2003), Changes in transitional snowfall season length in northern Eurasia, *Geophys. Res. Lett.*, *30*(5), 1252, doi:10.1029/2003GL016873.

Ye, H., H. Cho, and P. Gustafson (1998), The changes of Russian winter snow accumulation during 1936–1983 and its spatial patterns, *J. Clim.*, *11*, 856–863, doi:10.1175/1520-0442(1998)011<0856:TCIRWS>2.0.CO;2.

Ye, H., D. Yang, and D. Robinson (2008), Winter rain on snow and its association with air temperature in northern Eurasia, *Hydrol. Processes*, *22*(15), 2728–2736, doi:10.1002/hyp.7094.